THE BELL SYSTEM TECHNICAL JOURNAL
Vol. 58, No. 5, May–June 1979
*Printed in U.S.A.*

# Transmission Properties of Various Styles of Printed Wiring Boards

By A. J. RAINAL

(Manuscript received October 18, 1978)

*This paper presents some experimental results concerning the pulse transmission properties of fine line printed conductors (e.g., width = 8 mils, spaces = 9 mils) on various styles of circuit packs (CPs). The pulse transmission properties include the characteristic impedance, the propagation delay, the rise time, the bandwidth, and the intralayer and interlayer pulse crosstalk. A simplified theoretical model is presented which leads directly to some basic crosstalk equations. Theoretical results are developed to extend the application of the experimental crosstalk results to arbitrary pulse signals, periodic signals, and random signals. Also, theoretical scaling laws are developed to extend the crosstalk results to conductor spaces in the range of 7 to 40 mils. The crosstalk results are very important, since they tend to limit the packaging density of printed conductors on the CP styles by limiting the coupled length and spacing of parallel conductors. The results can be incorporated into computer-aided designs which can analyze routed CPs to detect potential crosstalk problems before the CP routing is finalized for manufacture. Other applications include CP selection, crosstalk estimation, electrical characterization of CPs and backplanes, estimation of conductor capacitance and inductance, and effects of various dielectrics. The results are applicable to general styles of printed wiring boards. In particular, they apply directly to all styles of CPs in the* BELLPAC™ *apparatus housing—a modular packaging system for packaging electronic equipment in the Bell System.*

## I. INTRODUCTION

In the physical design of large electronic systems, the interconnection of the integrated circuits and other components at the circuit pack or printed wiring-board level constitutes a basic and relatively expensive level of interconnection. In addition to supplying power and ground, the circuit pack (CP) provides the conductor paths for the

Table I—Description of the circuit pack styles

| Circuit Pack Style | Description |
|---|---|
| Wire wrap | Wire wrap board for breadboarding |
| Extender board | 6 layer MLB, 2 pad layers, 2 signal layers, power (P) and ground (G) on inside, dedicated ground conductor between every pair of signal conductors |
| Double-sided (epoxy) | Double-sided, epoxy PWB |
| Double-sided (metal) | Double-sided, metal core, PWB |
| Bonded board (LAMPAC)† | Flex bonded to epoxy coated steel |
| 4L MLB (EXT P/G) | 4 layer MLB, 2 signal layers, P and G on outside |
| 6L MLB (EXT P/G) | 6 layer MLB, 4 signal layers, P and G on outside |
| 6L MLB (INT P/G) | 6 layer MLB, 2 pad layers, 2 signal layers, P and G on inside |
| 6L MLB (INT P/G, surface routing) | 6 layer MLB, 4 signal layers, P and G on inside |
| 8L MLB (INT P/G) | 8 layer MLB, 2 pad layers, 4 signal layers, P and G on inside |

† This particular bonded board is also known as LAMPAC.

transmission of pulses and other types of signals between the integrated circuits, other components, and the CP connector.

The basic pulse transmission properties, such as characteristic impedance, propagation delay, rise time, bandwidth, and crosstalk depend a great deal on the CP configuration or style. Since the costs associated with the various CP styles differ significantly, it is very important to develop CP styles which are suitable electrically and which are relatively inexpensive.

For the past few years, a Bell System packaging effort[1] (*BELLPAC** packaging system) has been under way to develop a modular packaging system for packaging electronic equipment. This effort makes use of a suitable connector (963) and a number of CP styles that have common features suitable for computer-aided design.

The purpose of this paper is to present some basic transmission properties of various styles of CPs which include those in the *BELLPAC* hardware family. The transmission properties are very important, since they help to determine which CP style is most appropriate for a given application.

A listing of the CP styles along with a short description of each is presented in Table I. Copper conductors are used on all the CP styles. The dielectric material for most CPs is a composite of epoxy and glass fibers. The composite structure has a relative dielectric constant (effective) of about 4.2. Except for the extender board, all the CP styles have the common features shown in Fig. 1.

* Trademark of Western Electric.

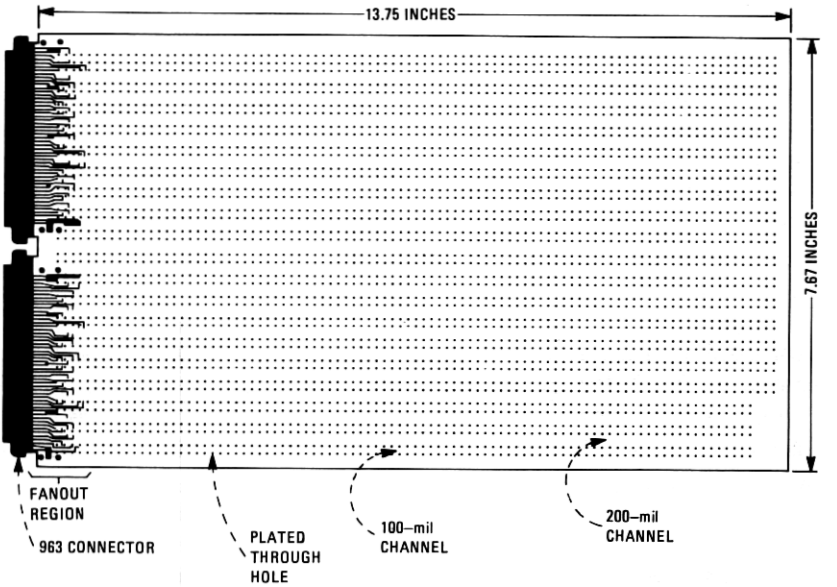


Fig. 1—Some common features applying to all circuit pack styles except the extender board. The plated-through holes are on either 100-mil or 200-mil centers. The spaces between the rows of plated-through holes are denoted as 100-mil or 200-mil channels.

The extender board is a very special design. Its primary function is to extend any CP beyond the apparatus housing so that both sides of the CP are accessible for debugging or test purposes. Thus, the extender board is basically an "extension cord" for a CP.

To determine the basic transmission properties of the various CPs, appropriate test boards were designed for each style of CP listed in Table I. Except for the double-sided (metal) board, all test boards were fabricated at the Western Electric printed-circuit manufacturing plant at Richmond, Virginia. The double-sided metal board was manufactured at the Western Electric plant in Kearny, New Jersey. The test routing consisted of either 8 ± 2 mil conductors with nominal 9-mil spaces or 12 ± 3 mil conductors with nominal 13-mil spaces. The 8-mil conductors were on 17-mil centers, and the 12-mil conductors were on 25-mil centers. In general, the length of the conductor paths was about 1 foot.

An experimental approach was necessary for this study because detailed theoretical models which include all CP styles of interest become very complicated, and they are not now very useful for determining many basic pulse transmission properties. The experimental methods used to determine the transmission properties of the test boards are described in the next section.

## II. DESCRIPTION OF THE EXPERIMENTAL METHODS

### 2.1 Pulse transmission properties

Each CP style containing the test routing was probed with a Hewlett Packard time domain reflectometer (TDR) system consisting of a 1815A sampling plug-in, an 1817A sampling head, and an 1106B tunnel diode pulse generator. The TDR system was used to apply a fast rising step signal into each CP and display the reflected waveform on a sampling oscilloscope. In general, the conductor path on the CP was open-circuited and was free of any parallel branches.

For purposes of detailed analysis, a photograph was taken of each TDR display of interest. The general form of the TDR display is presented in Fig. 2. By analyzing the TDR display of the reflected waveform, one can determine the basic pulse transmission properties of the various CP styles. The particular CP properties of interest are the characteristic impedance, $Z_1$, the propagation delay, $T_d$, the 80-percent rise time, $T_r$, and the bandwidth, $B$. All these CP properties can be determined by analyzing each TDR display as indicated in Fig. 2. The 80-percent rise time, $T_r$, on the TDR display is a result of the input step signal traversing the CP twice, as is characteristic of a reflection method. The one-way rise time is faster by a factor of approximately $1/\sqrt{2}$. By applying this factor to the usual relationship between bandwidth and rise time, we have

$$B = \frac{0.35}{T_r/\sqrt{2}} \doteq \frac{1}{2T_r}. \tag{1}$$

Reference 2 presents some additional discussion concerning the TDR method along with some detailed results concerning the theoretical TDR display for an ideal CP.

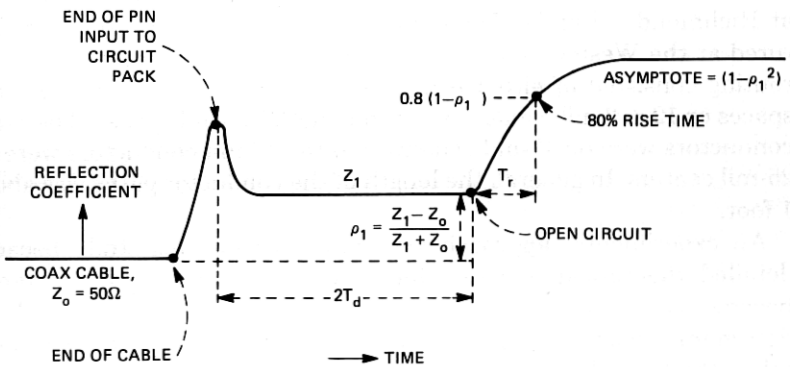


Fig. 2—The general form of the TDR display.

### 2.2 Pulse crosstalk properties

The pulse crosstalk properties of the CPs were determined experimentally by using the method described in Refs. 3, 4, and 5. Briefly, the method consists of applying a fast pulse (rise time ~ 2 ns) to a driven conductor and monitoring the resultant waveform at the near-end or far-end of some idle conductor of interest. In all cases, the crosstalk results apply when all conductors are properly terminated with matched loads. The corresponding results for other loads can yield higher values of crosstalk which can be estimated from the results for matched loads by determining the reflections and using superposition. Thus, the crosstalk results for the matched loads are basic properties of the CP styles. The crosstalk results are very important since they limit the packaging density of printed conductors on the CPs by limiting the coupled length and spacing of parallel conductors.

We now summarize all the experimental results presented in the appendix to this paper.

## III. SUMMARY OF THE EXPERIMENTAL RESULTS

Table II presents a summary of the pulse transmission properties of all the CPs considered in this paper. More detailed properties for each of the CP styles are presented in the appendix, as stated in the last column of Table II.

The propagation delay per foot, the rise time, and the bandwidth include the effects of the 963 connector plus fanout (see Fig. 1). However, an earlier study[6] has shown that the 963 connector plus fanout limits all the CP styles to applications having one-way signal rise times ($= 1/\sqrt{2}$ of the TDR rise time values) no faster than about 2.0 ns (bandwidths $\leq$ 175 MHz). This 2.0-ns limit was determined by considering the crosstalk levels and impedance mismatch associated with the 963 connector plus fanout. This lower limit on signal rise time is sufficient to include most applications in the Bell System.

The pulse crosstalk results were measured as a percentage of the signal step in the driven conductor. The crosstalk results apply when the printed conductors are terminated with matched loads.

The interlayer crosstalk can be decreased to negligible values by simply using orthogonal routing on adjacent layers. This technique is now widely used during the routing of the conductors. Therefore, intralayer crosstalk is usually more of a concern than is interlayer crosstalk.

The attenuation of the conductors has not been thoroughly investigated, but some preliminary results have shown that signal attenuation is about 0.4 dB/ft at 250 MHz.

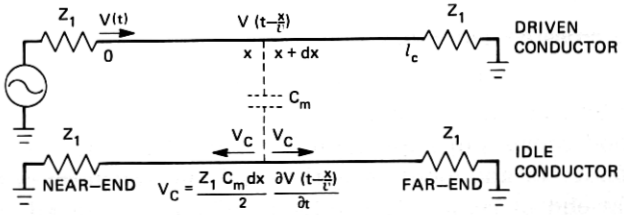


(a)

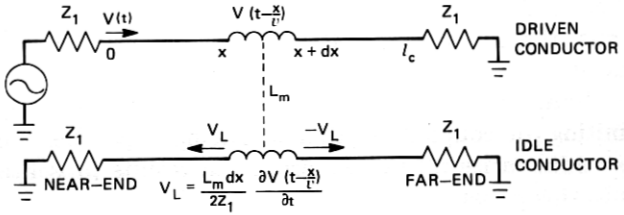


(b)

Fig. 3—A simplified model of crosstalk for a pair of lossless, uniformly, and loosely coupled conductors terminated with matched loads. $Z_1$, $v$, and $l_c$ denote characteristic impedance, propagation velocity, and coupled length, respectively. (a) Capacitive crosstalk, $V_c$, resulting from the mutual capacitance per unit length, $C_m$. (b) Inductive crosstalk, $V_L$, resulting from the mutual inductance per unit length, $L_m$.

Table II shows that the CP styles in the *BELLPAC* family of CPs* provide a wide variety of pulse transmission properties that can satisfy the CP needs of most presentday Bell System projects. Many current projects (e.g., AMARC, PDT2A, PLAID, Triport, ESS Ring and Tone, DIF) make use of the double-sided (epoxy) style. In fact, this is the most common CP style. The double-sided metal CP is used in customer equipment and is now under consideration for power supply applications. The 4L MLB and 6L MLB (EXT P/G) were used in some switching applications such as the PROCON project. The higher capability MLBs, the 6L MLBs (INT P/G with and without surface routing), were used in the 1A ESS processor, and are expected to find use in projects such as the 3B ESS processor and DIF.

## IV. THEORETICAL CROSSTALK RESULTS

### 4.1 Derivation of basic crosstalk equations

Consider the simplified model of crosstalk presented in Fig. 3. The capacitive crosstalk voltage denoted by $V_c$ in Fig. 3a is a suitable approximation when the conductors are loosely coupled. A more

* At the present time, the bonded board (LAMPAC) and the 8L MLB (INT P/G) are not members of the *BELLPAC* family of CP's.

Table II—Summary of pulse transmission properties of various circuit pack styles

| Circuit Pack Style | Characteristic Impedance (ohms) | Propagation delay* (ns per ft) | Rise time* (TDR) (ns) | Bandwidth* (MHz) | Maximum† Interlayer Pulse Crosstalk (Near-End) (percent) | Maximum† Intralayer Pulse Crosstalk (Near-End) (percent) | More Details Shown in the Following Figures in the Appendix |
|---|---|---|---|---|---|---|---|
| Wire wrap‡ | 125 ± 50 | 1.4 | 2.0 | 250 | — | 40 | 4 |
| | 160 ± 35 | 1.3 | 1.8 | 278 | | 35 | |
| Extender Board | 70 ± 5 | 1.8 | 1.3 | 385 | 0.3 | 1.6 | 5 |
| Double-Sided (epoxy)§ | 150 ± 20 | 1.5 | 2.6 | 190 | 21 | 39 | 6 |
| | 150 ± 20 | 1.5 | 2.6 | 190 | 24 | 34 | |
| Double-Sided (metal)§ | 98 ± 8 | 1.5 | 2.6 | 190 | 1.2 | 15 | 7 |
| | 83 ± 6 | 1.5 | 2.6 | 190 | 3.2 | 13 | |
| Bonded Board§ | 95 ± 10 | 1.5 | 2.6 | 190 | 38 | 21 | 8 |
| (LAMPAC) | 85 ± 10 | 1.5 | 2.6 | 190 | 44 | 19 | |
| 4L MLB | 95 ± 35 | 1.8 | 2.5 | 200 | 20 | 30 | 9 |
| (EXT P/G)§ | 85 ± 30 | 1.8 | 2.5 | 200 | 21 | 16 | |
| 6L MLB | 75 ± 30 | 1.8 | 2.5 | 200 | 40 | 32 | 10 |
| (EXT P/G)§ | 70 ± 35 | 1.8 | 2.5 | 200 | 46 | 16 | |
| 6L MLB | 68 ± 3 | 1.9 | 1.8 | 278 | 0.5 | 20 | 11 |
| (INT P/G)§ | 61 ± 3 | 1.9 | 1.8 | 278 | 0.5 | 15 | |
| 6L MLB | 85 ± 25 | 1.5 (surface), 1.8 | 1.8 | 278 | 22 | 16 | 12 |
| (INT P/G, Surface Routing)§ | 75 ± 15 | 1.5 (surface), 1.8 | 1.8 | 278 | 26 | 14 | |
| 8L MLB | 85 ± 25 | 1.9 | 1.8 | 278 | 20 | 18 | 13 |
| (INT P/G)§ | 75 ± 15 | 1.9 | 1.8 | 278 | 24 | 12 | |

* Includes the effect of 963 connector plus fanout; see Fig. 1.

† Maximum pulse crosstalk occurs when the round trip propagation delay over the coupled length is at least as great as the signal rise time. See Section 4.2.

‡ The first entry applies to Milene (registered trademark of W. L. Gore & Assoc., Inc.) insulation, the second to Teflon (registered trademark of E. I. DuPont) insulation.

§ The first entry applies to conductor width = 8 mils, conductor space = 9 mils, the second to 12, 13 mils.

accurate expression for $V_c$ is obtained by applying circuit theory to the elemental circuit in Fig. 3a. The result is that $V_c$ satisfies

$$\frac{dV_c}{dt} + \frac{V_c}{Z_1 C_m} = \frac{1}{2}\frac{\partial V(t - (x/v))}{\partial t} \tag{2}$$

or

$$V_c = \frac{1}{2}\int_{(x/v)}^{t} e^{-\frac{(t-\xi)}{Z_1 C_m}} \frac{\partial V(\xi - (x/v))}{\partial \xi} d\xi. \tag{3}$$

When the conductors are loosely coupled, $C_m$ is relatively small, and eq. (3) yields the approximation given in Fig. 3a, since

$$V_c = \frac{Z_1 C_m}{2}\int_{(x/v)}^{t} \frac{e^{-\frac{(t-\xi)}{Z_1 C_m}}}{Z_1 C_m} \frac{\partial V(\xi - (x/v))}{\partial \xi} d\xi \sim \frac{Z_1 C_m}{2}\frac{\partial V(t - (x/v))}{\partial t}. \tag{4}$$

The loose coupling approximation not only allows the simplification of $V_c$ but also allows one to neglect the interaction of the idle conductor on the driven conductor. When this interaction is considered along with conductor losses, the analysis becomes extremely difficult (see, for example, Refs. 7 and 8).

Using this simplified model, the total near-end (backward) crosstalk waveform, $V_{ne}(t)$, and the total far-end (forward) crosstalk waveform, $V_{fe}(t)$, can be expressed as two independent differential equations:

$$dV_{ne}(t) = \frac{1}{2}\left(Z_1 C_m + \frac{L_m}{Z_1}\right) dx \frac{\partial V(t - (2x/v))}{\partial t} \tag{5}$$

$$dV_{fe}(t) = \frac{1}{2}\left(Z_1 C_m - \frac{L_m}{Z_1}\right) dx \frac{dV(t - (l_c/v))}{dt}. \tag{6}$$

By integrating the variable $x$ over the coupled length $l_c$, we have that

$$V_{ne}(t) = \frac{1}{2}\left(Z_1 C_m + \frac{L_m}{Z_1}\right)\int_0^{l_c} \frac{\partial V(t - (2x/v))}{\partial t} dx \tag{7}$$

$$= K_{ne}[V(t) - V(t - 2T_D)], \tag{8}$$

where

$$T_D = \frac{l_c}{v} = \text{propagation delay over the coupled length}$$

$$K_{ne} = \frac{v}{4}\left[Z_1 C_m + \frac{L_m}{Z_1}\right].$$

Similarly,

$$V_{fe}(t) = \frac{1}{2}\left(Z_1C_m - \frac{L_m}{Z_1}\right)\int_0^{l_c} \frac{dV(t - T_D)}{dt}\,dx \tag{9}$$

$$= K_{fe}l_c \frac{dV(t - T_D)}{dt}, \tag{10}$$

where

$$K_{fe} = \frac{1}{2}\left(Z_1C_m - \frac{L_m}{Z_1}\right).$$

Equations (8) and (10) agree with the earlier results presented in Refs. 3, 4, 9, 10, 11, and 12. These references also contain some useful discussions of crosstalk associated with printed wiring interconnections.

Notice that, if $Z_1C_m = (L_m/Z_1)$, $K_{fe} \equiv 0$ and $V_{fe}(t) = 0$. This result forms the basis of the design of directional couplers and occurs quite naturally whenever the conductors are surrounded by a homogeneous medium. See Ref. 13 for a discussion of this interesting point. However, for all the CPs considered in this paper, it turns out that $V_{fe}(t) \neq 0$.

The simplified model presented in Fig. 3 can be generalized to include the case when the driven conductor has characteristic impedance $Z_1$ and propagation velocity $v_1$ while the idle conductor has characteristic impedance $Z_2$ and propagation velocity $v_2$. For this case, (5) and (6) become:

$$dV_{ne}(t) = \frac{1}{2}\left(Z_2C_m + \frac{L_m}{Z_1}\right)dx \frac{\partial V\left(t - \frac{x}{v_1} - \frac{x}{v_2}\right)}{\partial t} \tag{11}$$

$$dV_{fe}(t) = \frac{1}{2}\left(Z_2C_m - \frac{L_m}{Z_1}\right)dx \frac{\partial V\left[t - \frac{x}{v_1} - (l_c - x)/v_2\right]}{\partial t}. \tag{12}$$

By integrating the variable $x$ over the coupled length $l_c$, we have

$$V_{ne}(t) = \frac{1}{2}\left(Z_2C_m + \frac{L_m}{Z_1}\right)\left(\frac{v_1v_2}{v_1 + v_2}\right) \cdot\left\{V(t) - V\left[t - l_c\left(\frac{v_1 + v_2}{v_1v_2}\right)\right]\right\} \tag{13}$$

$$V_{fe}(t) = \frac{1}{2}\left(Z_2C_m - \frac{L_m}{Z_1}\right)\left(\frac{v_1v_2}{v_2 - v_1}\right) \cdot\left\{V\left(t - \frac{l_c}{v_2}\right) - V\left(t - \frac{l_c}{v_1}\right)\right\}. \tag{14}$$

Equations (13) and (14) agree with the results given in Ref. 11, and they reduce to (8) and (10) when $Z_2 = Z_1$ and $v_1 = v_2 = v$.

The corresponding results for the case when the driven conductor has $Z_2$, $v_2$ and the idle conductor has $Z_1$, $v_1$ can be obtained from eqs. (13) and (14) merely by interchanging $Z_1$ and $Z_2$ and also $v_1$ and $v_2$. In this manner, one can determine the following general result:

$$\frac{V_{ne}(t, Z_2, v_2)}{V_{ne}(t, Z_1, v_1)} = \frac{V_{fe}(t, Z_2, v_2)}{V_{fe}(t, Z_1, v_1)} = \frac{Z_2}{Z_1}, \tag{15}$$

where

$V_{ne}(t, Z_i, v_i)$ = near-end crosstalk waveform when the idle conductor has $Z_i$, $v_i$,

and

$V_{fe}(t, Z_i, v_i)$ = far-end crosstalk waveform when the idle conductor has $Z_i$, $v_i$.

Notice that eq. (15) is independent of time and the propagation velocities. Also, it can be shown that (15) satisfies reciprocity.

In CP design, one usually attempts to make the characteristic impedance constant throughout the CP or $Z_1 = Z_2$. However, if $Z_1 \neq Z_2$ (as it can be when dealing with interlayer crosstalk), then eq. (15) shows that both near-end and far-end crosstalk are reduced when the conductor having the lower characteristic impedance is taken as the idle conductor.

Although eqs. (13) and (14) are more general, experimental work has shown that eqs. (8) and (10) or, more generally, eqs. (13) and (14) with $v_1 = v_2 = v$ are sufficient for characterizing the crosstalk on all the CP styles of interest in this paper. Also, in order to help simplify the tables in the appendix, we shall only report on the average interlayer crosstalk associated with a given conductor pair. This appears to be sufficient, since interlayer crosstalk is usually of less concern than intralayer crosstalk.

The results based on the simplified model given in Fig. 3 turn out to be good approximations for printed wiring boards when the value of $K_{ne}$ is less than about 25 percent. However, even when $K_{ne}$ is somewhat greater than 25 percent, the results based on the simplified model can still be applied, although they become less accurate in this region.

On all styles of CPs, we have found experimentally that $\max |V_{fe}(t)| < \max V_{ne}(t)$ for all signals and coupled lengths of interest* in this paper. Thus, by controlling $V_{ne}(t)$, one also controls $V_{fe}(t)$. Accordingly, we have directed our experimental work toward estimating the magnitude of the near-end crosstalk and only provide experimental bounds on the intralayer far-end crosstalk for all the CP styles.

* Because of connector limitations, the signal rise times of interest are 2 ns or more (i.e., a signal bandwidth of 175 MHz or less). The coupled lengths of interest are all less than 18 inches.

### 4.2 Crosstalk resulting from a pulse signal

Let $V(t)$ represent a ramp type of pulse signal given by:

$$V(t) = \begin{cases} \dfrac{V_o t}{T_R}, & 0 \le t \le T_R \\ V_o, & t > T_R. \end{cases} \tag{16}$$

When $V_o > 0$, $V(t)$ represents a rising step signal having a 100 percent rise time of $T_R$. This type of signal is convenient for characterizing the crosstalk resulting from the leading edge of a pulse signal.

In practice, the total near-end crosstalk, NEXT, is usually defined as the fraction of the pulse drive signal that appears at the near-end of the idle conductor. Thus, for the pulse signal, eq. (8) yields:

$$\text{NEXT} = \frac{\max V_{ne}(t)}{V_0} = \begin{cases} K_{ne}, & 2T_D > T_R \\ K_{ne}\left(\dfrac{2T_D}{T_R}\right), & 2T_D \le T_R. \end{cases} \tag{17}$$

When $2T_D > T_R$, the near-end waveform, $V_{ne}(t)$, is a trapezoidal pulse and when $2T_D \le T_R$, this waveform is a triangular pulse.

Equation (17) shows that the value of $K_{ne}$ represents the maximum value of near-end pulse crosstalk. In the appendix, the experimental values of $K_{ne}$ and $1/v = T_D/l_c$ for all CPs of interest in this paper are tabulated in Tables A and B of Figs. 4 through 13. By using these tabulated values and eq. (17), one can readily estimate the NEXT for an arbitrary pulse-like signal on any CP style.

As discussed in Section 4.1, only the average values of $K_{ne}$ for interlayer, near-end crosstalk are tabulated. To estimate the two individual values of $K_{ne}$ for interlayer, near-end crosstalk, it can be shown that each $K_{ne}$ value must be multiplied by $\sqrt{Z_1/Z_2}$ and $\sqrt{Z_2/Z_1}$. The values of $Z_1$, $Z_2$, the characteristic impedances of the conductors, are also tabulated in the appendix.

The corresponding result for the total far-end crosstalk, FEXT, can be obtained from eq. (10):

$$\text{FEXT} = \frac{\max |V_{fe}(t)|}{V_o} = \frac{|K_{fe}|\, l_c}{T_R}. \tag{18}$$

In this case, the far-end crosstalk waveform, $V_{fe}(t)$, is a rectangular pulse.

For all the CP styles, we have determined experimentally that $|K_{fe}| \le 0.09$ ns/ft for intralayer crosstalk. We shall see that this result can be used to bound intralayer FEXT on all the CPs.

### 4.3 Crosstalk resulting from a periodic signal

If $V(t)$ represents a periodic signal of period $T = 1/f_o$, then

$$V(t) = \sum_{n=-\infty}^{\infty} \alpha_n e^{i\omega_n t}, \tag{19}$$

where

$$\alpha_n = \frac{1}{T}\int_{-T/2}^{T/2} V(t)\, e^{-i\omega_n t}\, dt$$

and

$$\omega_n = n2\pi f_o.$$

For this periodic signal, eq. (8) yields

$$V_{ne}(t) = K_{ne} \sum_{n=-\infty}^{\infty} (2i\alpha_n \sin \omega_n T_D) e^{i\omega_n (t-T_D)}. \tag{20}$$

If we now define near-end crosstalk, NEXT, as

$$\text{NEXT} \equiv \left[\frac{\text{ac power of } V_{ne}(t)}{\text{ac power of } V(t)}\right]^{1/2}, \tag{21}$$

then

$$\text{NEXT} = 2K_{ne}\left[\frac{\sum_{n=1}^{\infty} |\alpha_n \sin \omega_n T_D|^2}{\sum_{n=1}^{\infty} |\alpha_n|^2}\right]^{1/2} \leq 2K_{ne}. \tag{22}$$

Equation (22) shows that NEXT $\leq 2K_{ne}$ for all periodic signals.

The corresponding result for FEXT, assuming no jump discontinuities in $V(t)$, is

$$V_{fe}(t) = K_{fe} l_c \sum_{n=-\infty}^{\infty} i\alpha_n \omega_n e^{i\omega_n (t-T_D)} \tag{23}$$

and

$$\text{FEXT} \equiv \left[\frac{\text{ac power of } V_{fe}(t)}{\text{ac power of } V(t)}\right]^{1/2} \tag{24}$$

$$= |K_{fe}|\, l_c \left[\frac{\sum_{n=1}^{\infty} |\alpha_n \omega_n|^2}{\sum_{n=1}^{\infty} |\alpha_n|^2}\right]^{1/2}. \tag{25}$$

By using the tabulated values of $K_{ne}$ and $1/v = T_D/l_c$ given in the appendix together with eq. (22), one can estimate the NEXT resulting

from a general periodic signal on any of the CPS. Also, by using the bound on $|K_{fe}|$ given in Section 4.2 along with eq. (25), one can bound the intralayer FEXT on any of the CPS.

As an example of a simple periodic signal, let $V(t)$ represent a sinusoid of frequency $f_o$. Then eqs. (22) and (25) yield

$$\text{NEXT} = 2K_{ne}|\sin 2\pi f_o T_D| \tag{26}$$

$$\text{FEXT} = |K_{fe}| l_c 2\pi f_o. \tag{27}$$

When $f_o = (4T_D)^{-1}$, NEXT attains its maximum value of $2K_{ne}$, which is twice the maximum NEXT resulting from the pulse signal considered in Section 4.2.

It can be shown that eqs. (26) and (27) are special cases of the more general results presented in the classical works on sinusoidal crosstalk presented in Refs. 14 and 15. These references also include the effects of conductor losses. In our application, the coupled length, $l_c$, is relatively short ($l_c \leq 18''$), so that conductor losses are negligible over a frequency range of about 250 MHz.

For small values of $f_o T_D (= f_o l_c / v)$, eq. (26) yields

$$\text{NEXT} = 4\pi K_{ne} f_o T_D = 4\pi K_{ne} \frac{f_o l_c}{v}. \tag{28}$$

In this case, eq. (28) shows that NEXT is proportional to both frequency, $f_o$, and coupled length $l_c$ much as is FEXT.

### 4.4 Crosstalk resulting from a random signal

Let $V(t)$ represent a differentiable, stationary random signal having zero mean and one-sided power spectral density $W(f)$. The correlation function, $\rho(\tau)$, of the random signal is defined by

$$\rho(\tau) = E[V(t)V(t+\tau)] = \int_0^\infty W(f) \cos 2\pi f\tau \, df, \tag{29}$$

where $E$ = expectation operator.

The correlation function, $\rho_{ne}(\tau)$, of the crosstalk waveform at the near-end of the idle conductor can be determined from eq. (8). Thus,

$$\begin{aligned}\rho_{ne}(\tau) &= E[V_{ne}(t)V_{ne}(t+\tau)] \\ &= K_{ne}^2[2\rho(\tau) - \rho(\tau - 2T_D) - \rho(\tau + 2T_D)].\end{aligned} \tag{30}$$

The power spectral density, $W_{ne}(f)$, of $V_{ne}(t)$ is given by

$$W_{ne}(f) = 4\int_0^\infty \rho_{ne}(\tau) \cos 2\pi f\tau \, d\tau \tag{31}$$

$$= 4K_{ne}^2 W(f) \sin^2 2\pi f T_D. \tag{32}$$

For this random signal case, it is reasonable to define the NEXT by

$$\text{NEXT} = \frac{\sigma_{ne}}{\sigma}, \tag{33}$$

where

$\sigma_{ne}$ = rms value of $V_{ne}(t)$

$\sigma$ = rms value of $V(t)$.

Thus,

$$\text{NEXT} = \frac{\sigma_{ne}}{\sigma} = \sqrt{\frac{\rho_{ne}(0)}{\rho(0)}} \tag{34}$$

$$= \sqrt{2}K_{ne}\left[1 - \frac{\rho(2T_D)}{\sigma^2}\right]^{1/2} \leq 2K_{ne}. \tag{35}$$

Equation (35) shows that NEXT is bounded by $2K_{ne}$ for all stationary random signals.

The corresponding results at the far end are

$$\rho_{fe}(\tau) = E[V_{fe}(t)V_{fe}(t+\tau)] = -|K_{fe}|^2 l_c^2 \rho''(\tau) \tag{36}$$

$$W_{fe}(f) = [|K_{fe}|\, l_c(2\pi f)]^2 W(f) \tag{37}$$

and

$$\text{FEXT} = \frac{\sigma_{fe}}{\sigma} = |K_{fe}|\, l_c \sqrt{\frac{-\rho''(0)}{\rho(0)}} \tag{38}$$

$$= |K_{fe}|\, l_c \pi \beta, \tag{39}$$

where

$\sigma_{fe}$ = rms value of $V_{fe}(t)$

$\beta$ = average number of zero crossings per second of $V(t)$.

Thus, for all differentiable, stationary random signals FEXT is proportional to the average number of zero crossings per second of $V(t)$.

By using the tabulated values of $K_{ne}$ and $1/v(= T_D/l_c)$ given in the appendix together with eq. (35), one can estimate the NEXT resulting from a general random signal on any of the CPs. Also, by using the bound on $|K_{fe}|$ given in Section 4.2 along with eq. (38), one can bound the intralayer FEXT on any of the CPs.

As an example of a random signal, let

$$W(f) = \begin{cases} \dfrac{\sigma^2}{B}, & f_o - \dfrac{B}{2} \leq f \leq f_o + \dfrac{B}{2} \\ 0, & \text{otherwise,} \end{cases} \tag{40}$$

where

$B$ = bandwidth of the signal $V(t)$

$f_o$ = center frequency of the signal $V(t)$.

For this case, eqs. (29) and (35) yield

$$\text{NEXT} = \frac{\sigma_{ne}}{\sigma} = \sqrt{2}K_{ne}\left[1 - \left(\frac{\sin 2\pi BT_D}{2\pi BT_D}\right)\cos 4\pi f_o T_D\right]^{1/2}. \quad (41)$$

Notice that, as $B \to 0$, eq. (41) approaches eq. (26), the corresponding result for the sine wave case.

The result for FEXT is

$$\text{FEXT} = \frac{\sigma_{fe}}{\sigma} = |K_{fe}|\, l_c \pi \sqrt{4f_0^2 + B^2/3}. \quad (42)$$

As $B \to 0$, this result approaches eq. (27), the corresponding result for the sine wave case.

The theoretical developments in Sections 4.2, 4.3, and 4.4 can be generalized to include eqs. (13) and (14) in place of eqs. (8) and (10). When $v_1 = v_2 = v$, all one needs to do is replace $Z_1C_m$ by $Z_2C_m$ in $K_{ne}$ and $K_{fe}$. The more general case, $v_1 \neq v_2$, will not be treated in this paper, since experimental results show that the propagation velocity is approximately constant on a given CP.

## V. SOME APPLICATIONS

### 5.1 Selection of a CP style

Since the costs associated with the various CP styles differ significantly,[1] it is very important to select a CP style which is both suitable electrically and relatively inexpensive. The pulse transmission properties summarized in Table II and tabulated in more detail in the appendix can be used to help select such a cost-effective CP for a given application.

It is also very important that the physical designers and systems designers using *BELLPAC* hardware be aware of these basic pulse transmission properties. The CP transmission properties must be compatible with the transmission properties of the backplane, frame wiring, and the CP components.

### 5.2 Estimation of crosstalk on a given CP style

By using the theoretical results presented in Section IV together with the appropriate $K_{ne}$ and $1/v$ values given in the appendix, one can estimate the amount of near-end crosstalk for fine line conductors carrying a wide variety of signals on any of the CPs considered in this paper. As discussed in Section IV, far-end crosstalk is always less

than near-end crosstalk, usually much less. Also, intralayer, far-end crosstalk can be bounded by using the experimentally determined constant $|K_{fe}| \leq 0.09$ ns/ft and the theoretical results presented in Section IV.

Let us consider as an example a pair of adjacent, parallel conductors on the inside signal layer of the 6L MLB (INT P/G, surface routing). From Table B of Figure 12 in the appendix, we see that $K_{ne} = 0.16$ for two adjacent conductors ($Y_1 Y_2$) in the 200-mil channel when the conductor width and conductor spacing are 8 and 9 mils, respectively. Table A of this same figure gives $1/v = 1.8$ ns/ft. Thus, for a pulse signal, eq. (17) yields

$$\text{NEXT} = \begin{cases} 0.16, & 2T_D > T_R \\ (0.16)\left(\dfrac{2T_D}{T_R}\right), & 2T_D \leq T_R, \end{cases} \tag{43}$$

where

$T_D = \dfrac{l_c}{v}$ = propagation delay over the coupled length (ns)

$l_c$ = coupled length (ft)

$T_R$ = rise time of the pulse signal (ns).

Also, for the pulse signal, eq. (18) yields

$$\text{FEXT} \leq (0.09)\frac{l_c}{T_R}. \tag{44}$$

Similarly, for a sine wave signal of frequency $f_o$, eqs. (26) and (27) yield

$$\text{NEXT} = (2)(0.16)\,|\sin 2\pi f_o T_D| \tag{45}$$

$$\text{FEXT} \leq (0.09)\, l_c 2\pi f_o. \tag{46}$$

In a very similar manner, one can also estimate the NEXT and bound the intralayer FEXT for an arbitrary periodic or random signal by using eqs. (22), (25), (35), and (39).

By using this method, one can estimate the NEXT and bound the FEXT for a wide variety of conductor pairs and a wide variety of signal types on any of the CPs considered in this paper.

For a required crosstalk constraint, the theoretical and experimental crosstalk results can be used to help determine routing restrictions on coupled length for general types of signals. Alternately, this information can be incorporated into computer-aided designs to help determine whether a routed CP has violated a given crosstalk constraint associated with a particular signal type. In this manner, a routed CP

can be analyzed to detect potential crosstalk problems before the CP routing is finalized for manufacture.

As a final point concerning the estimate of crosstalk, one can also estimate intralayer NEXT for a pair of adjacent, parallel conductors having a range of conductor spacings. It turns out that intralayer NEXT is essentially independent of conductor width (see Ref. 4). Accordingly, to estimate the value of $K_{ne}(S)$ for a pair of adjacent, parallel conductors (i.e., $Y_1Y_2$) having conductor spacing $S$, one can interpolate or extrapolate the values of $K_{ne}$ for $S = 9$ mils or 13 mils given in the appendix by assuming that $K_{ne}(S)$ is proportional to $1/S$. It can be shown that this is a satisfactory assumption when 7 mils $\leq S \leq 40$ mils, the region of most interest in this paper.

As an example, let us apply this method to a pair of adjacent parallel conductors having conductor spacing $S$ (mils) on the inside signal layer of the 6L MLB (INT P/G, surface routing). For the 200-mil channel, Table B of Fig. 12 yields the following minimum mean square error estimate:

$$K_{ne}(S) = (9)(13)\frac{[13K_{ne}(9) + 9K_{ne}(13)]}{(9^2 + 13^2)S} = \frac{147.9}{S}\,\%. \qquad (47)$$

This method can be applied to pairs of adjacent, parallel conductors on any CP considered in this paper.

### 5.3 *Electrical comparison of the CPs*

The results in Table II and the appendix can be used to compare the various CPs from the electrical point of view. For example, Table II shows that, of the three CPs containing only two layers of metallization, namely, the double-sided epoxy, the double-sided metal, and the bonded board, the double-sided epoxy board is inferior to the other two. It has a relatively high characteristic impedance and higher values of intralayer crosstalk. Recall that intralayer crosstalk is more troublesome than interlayer crosstalk, which can be reduced considerably by using orthogonal routing on adjacent layers.

Also, the double-sided metal board is somewhat better electrically than the bonded board because the impedance variations and crosstalk are less for the metal board.

Table II also shows that the MLBs having an internal power and ground plane (INT P/G) are superior electrically to those having an external power and ground plane (EXT P/G). The MLBs having (INT P/G) have less impedance variations and yield less intralayer crosstalk.

Notice from Table II that a wire-wrap CP and the double-sided (epoxy) CP are both inferior to the MLB styles from the electrical point of view. Also, the double-sided (metal) and the bonded board have electrical properties which are comparable to all the MLBs having (INT P/G).

Finally, the extender board, because of its special design, is clearly the best electrical design of all the CPs considered in this paper. It has relatively little variation in characteristic impedance and very low crosstalk.

### 5.4 Estimation of the capacitance and inductance of the conductors

In certain applications of the CPs, it is important to have an estimate of the value of $C$, the capacitance per unit length, and $L$, the inductance per unit length for the conductors on all of the CP styles. This information is important, for example, when one needs to estimate the electrical load on a driver circuit for certain ranges of frequency or rise times. The values of $C$ and $L$ can be estimated from the values of propagation delay per foot $(1/v)$ and characteristic impedance $Z_1$ given in the appendix for each CP style. Using these values, $C$ and $L$ are given by

$$C = \frac{(1/v)}{Z_1} \frac{nf}{ft} \tag{48}$$

$$L = \left(\frac{1}{v}\right) Z_1 \frac{nh}{ft}. \tag{49}$$

For worst case estimates, $1/v$ should be increased by about 10 percent, since the values listed in the appendix are averages over about 20 different conductor paths on each CP.

### 5.5 Generalization to other dielectric materials

If eqs. (48) and (49) are used in eq. (8) to reduce $K_{ne}$, we have

$$K_{ne} = \frac{1}{4}\left[\frac{C_m}{C} + \frac{L_m}{L}\right]. \tag{50}$$

Equation (50) shows that $K_{ne}$ is independent of the relative dielectric constant, $\epsilon_r$ (effective). It can also be shown that the more general $K_{ne}$ discussed at the end of Section 4.4 is also independent of the relative dielectric constant. Thus, the values of $K_{ne}$ given in the appendix apply when the CPs are fabricated with any dielectric material.

One can also show that the propagation delay per foot, $1/v$, and the far-end crosstalk coefficient $|K_{fe}|$ are both proportional to $\sqrt{\epsilon_r}$, while the characteristic impedance, $Z_1$, is inversely proportional to $\sqrt{\epsilon_r}$. Thus, many of the results in this paper can be applied when the CPs are fabricated with other dielectric materials such as ceramic, Teflon, or polyimide.

### 5.6 Electrical characterization of backplanes

In the physical design of large electronic systems, various styles of printed wiring-board backplanes are often used to interconnect CPs.

These backplanes are usually very similar to some CP styles considered in this paper. Accordingly, many results in this paper can be applied to help electrically characterize various styles of backplanes.

## VI. SUMMARY

A Bell System packaging effort (*BELLPAC* packaging system) is now under way to develop a modular packaging system for packaging electronic equipment. This effort makes use of a suitable connector (963) and a number of circuit pack (CP) styles (ranging from wire-wrap CPs to multilayer board CPs) which have common features suitable for computer-aided design.

This paper presents some experimental results concerning the pulse transmission properties of fine line printed conductors (e.g., width = 8 mils, spaces = 9 mils) on various styles of CPs which include those in the *BELLPAC* hardware family of CPs. The pulse transmission properties include the characteristic impedance, the propagation delay, the rise time, the bandwidth, and the intralayer and interlayer pulse crosstalk. Theoretical scaling laws are developed to extend the application of the experimental crosstalk results to conductor spaces in the range of 7 to 40 mils.

A simplified theoretical model is presented which leads, directly, to some basic crosstalk equations. Also, theoretical results are developed to extend the application of the experimental crosstalk results to arbitrary pulse signals, periodic signals, and random signals.

The results in this paper can be applied to the:

(*i*) Selection of a CP style for a given application.
(*ii*) Estimation of crosstalk on a given CP style.
(*iii*) Comparison of the electrical properties of the CP styles.
(*iv*) Estimation of the capacitance and inductance of the conductors.
(*v*) Determination of the pulse transmission properties of the CP styles with various dielectrics.
(*vi*) Electrical characterization of various styles of backplanes.

The crosstalk results are very important since they tend to limit the packaging density of printed conductors on the CP styles by limiting the coupled length and spacing of parallel conductors.

## VII. ACKNOWLEDGMENTS

In the course of carrying out this program, the author received valuable support from A. G. Lubowe, A. P. Irwin, J. J. Waltz, H. B. Koons, M. P. Lum, W. H. Knausenberger, R. J. Stanzione, B. C. Fichter, R. A. Davis, and D. Dinella. The author also wishes to thank J. G. Brinsfield for some initial encouragement.

## APPENDIX

### *Experimental Results*

Index to pulse transmission properties

| Circuit Pack Style | Figure No. Containing the Pulse Transmission Properties |
|---|---|
| Wire wrap | 4 |
| Extender board | 5 |
| Double-sided (epoxy) | 6 |
| Double-sided (metal) | 7 |
| Bonded board (LAMPAC) | 8 |
| 4L MLB (EXT P/G) | 9 |
| 6L MLB (EXT P/G) | 10 |
| 6L MLB (INT P/G) | 11 |
| 6L MLB (INT P/G, surface routing) | 12 |
| 8L MLB (INT P/G) | 13 |

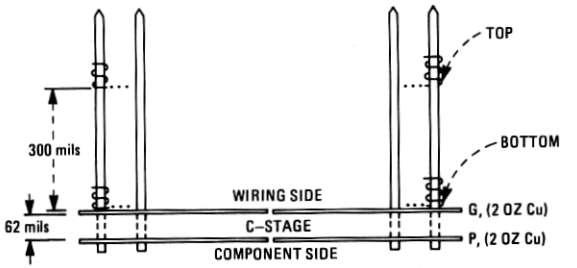


LAYUP FOR THE WIRE WRAP BOARD

**TABLE A**
**PULSE TRANSMISSION PROPERTIES OF THE WIRE WRAP BOARD**

| | AWG 30 WITH MILENE INSULATION | | AWG 30 WITH TEFLON INSULATION | |
|---|---|---|---|---|
| | LOCATION OF WRAP ON PIN | CHARACTERISTIC IMPEDANCE (OHMS) | LOCATION OF WRAP ON PIN | CHARACTERISTIC IMPEDANCE (OHMS) |
| ROUTING IN 200 mil CHANNELS(1) | TOP | 175 OHMS | TOP | 194 OHMS |
| | BOTTOM | 78 | BOTTOM | 124 |
| ROUTING IN 100 mil CHANNELS | TOP | 158 | TOP | 164 |
| | BOTTOM | 117 | BOTTOM | 138 |

- PROPAGATION DELAY = 1.4 ns/ft. (=1/v, MILENE), 1.3 ns/ft. (=1/v, TEFLON).
- 80% RISE TIME ON TDR FOR 1 ft CONDUCTOR LENGTH = 2.0 ns (MILENE) 1.8 ns (TEFLON).
- BANDWIDTH FOR 1 ft CONDUCTOR LENGTH = 250 MHz (MILENE), 278 MHz (TEFLON).

(1) THE 200 mil CHANNEL ALSO CONTAINS A GROUND PLANE.

**TABLE B**
**$K_{ne}$ = MAXIMUM NEAR–END PULSE CROSSTALK(1) FOR VARIOUS WIRE PAIRS ON THE WIRE WRAP BOARD**

| | AWG 30 WITH MILENE INSULATION | | AWG 30 WITH TEFLON INSULATION | |
|---|---|---|---|---|
| | LOCATION OF WRAP ON PIN | CROSSTALK (TIGHTLY COUPLED PAIRS) | LOCATION OF WRAP ON PIN | CROSSTALK (TIGHTLY COUPLED PAIRS) |
| ROUTING IN 200 mil CHANNELS(2) | TOP | 40 % | TOP | 35 % |
| | BOTTOM | 16 | BOTTOM | 23 |
| ROUTING IN 100 mil CHANNELS | TOP | 28 | TOP | 36 |
| | BOTTOM | 23 | BOTTOM | 13 |

(1) CROSSTALK WAS MEASURED AS A PERCENTAGE OF THE INPUT STEP.

(2) THE 200 mil CHANNEL ALSO CONTAINS A GROUND PLANE.

Fig. 4—Impedance, propagation delay, rise time, bandwidth, and pulse crosstalk for the wire-wrap board with 963C-100 connectors.

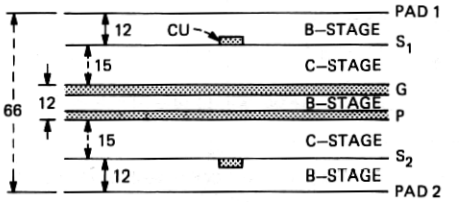


● 2 OZ CU CONDUCTORS ● ALL DIMENSIONS IN MILS

(a) NOTATION FOR INTERLAYER CROSSTALK ON THE EXTENDER BOARD.

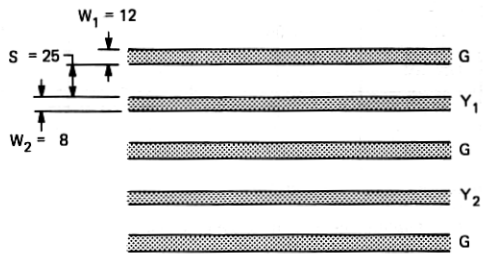


(b) NOTATION FOR INTRALAYER CROSSTALK ON THE EXTENDER BOARD.

**ELECTRICAL CHARACTERISTICS OF LARGEST (7.67" X 14.78") EXTENDER BOARD (WITH 963C CONNECTORS)**

- CHARACTERISTIC IMPEDANCE = 70 ± 5 OHMS.
- PROPAGATION DELAY = 1.80 ns/ft.
- 80 % RISE TIME ON TDR = 1.3 ns.
- BANDWIDTH = 385 MHz.
- MAXIMUM INTRALAYER NEXT: $Y_1$ $Y_2$ = 1.6 %
- MAXIMUM INTERLAYER NEXT: $S_1$ $S_2$ = 0.3 %

Fig. 5—Impedance, propagation delay, rise time, bandwidth, and pulse crosstalk for the extender board with 963C-100 connectors.

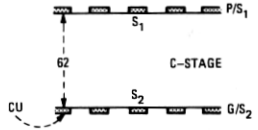


●2 OZ CONDUCTORS ●ALL DIMENSIONS IN MILS

(a) NOTATION FOR INTERLAYER CROSSTALK ON THE DOUBLE SIDED EPOXY PWB.

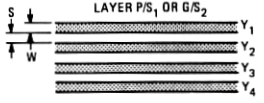


(b) NOTATION FOR INTRALAYER CROSSTALK. W = 12, S = 13 MILS OR W = 8, S = 9 MILS.

**TABLE A**
**PULSE TRANSMISSION PROPERTIES OF THE DOUBLE–SIDED EPOXY PWB[3]**

| | CONDUCTOR WIDTH = 12 mils CONDUCTOR SPACING = 13 mils | | CONDUCTOR WIDTH = 8 mils CONDUCTOR SPACING = 9 mils | |
|---|---|---|---|---|
| | SIGNAL LAYER | CHARACTERISTIC IMPEDANCE (OHMS) | SIGNAL LAYER | CHARACTERISTIC IMPEDANCE (OHMS) |
| ROUTING IN 200 mil CHANNELS[2] | $P/S_1$ | 163 OHMS | $P/S_1$ | 158 OHMS |
| | $G/S_2$ | 166 | $G/S_2$ | 163 |
| | $P/S_1 \rightarrow G/S_2$[1] | 146 | $P/S_1 \rightarrow G/S_2$ | 150 |
| ROUTING IN 100 mil CHANNELS | $P/S_1$ | 142 | $P/S_1$ | 142 |
| | $G/S_2$ | 135 | $G/S_2$ | 146 |
| | $P/S_1 \rightarrow G/S_2$ | 129 | $P/S_1 \rightarrow G/S_2$ | 129 |

- PROPAGATION DELAY = 1.5 ns/ft. (=1/v).
- 80% RISE TIME ON TDR FOR 1ft CONDUCTOR LENGTH = 2.6 ns.
- BANDWIDTH FOR 1ft CONDUCTOR LENGTH = 190 MHz.

(1) THE TRANSITIONS FROM $P/S_1$ TO $G/S_2$ USED 10 VIAS.

(2) THE P/G ROUTING ALSO OCCUPIES THE 200 mil CHANNELS.

(3) NO COVERCOAT CASE. COVERCOAT (GFR) HAS NEGLIGIBLE EFFECT ON RISE TIME (OR BANDWIDTH) BUT DECREASES THE CHARACTERISTIC IMPEDANCE BY ABOUT 5% AND INCREASES THE PROPAGATION DELAY BY ABOUT 10%.

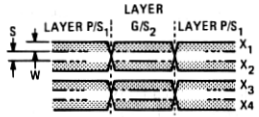


(c) NOTATION FOR CROSSTALK BETWEEN CONDUCTORS WHICH APPEAR ALTERNATELY ON LAYERS $P/S_1$ AND $G/S_2$. W = 12, S = 13 MILS OR W = 8, S = 9 MILS.

**TABLE B**
**$K_{ne}$ = MAXIMUM NEAR–END PULSE CROSSTALK[1] FOR VARIOUS CONDUCTOR PAIRS ON THE DOUBLE–SIDED EPOXY PWB[3]**

CONDUCTOR WIDTH = 12 mils, CONDUCTOR SPACING = 13 mils

| | INTERLAYER | INTRALAYER | | | | ALTERNATELY ON $P/S_1$, $G/S_2$ | | |
|---|---|---|---|---|---|---|---|---|
| LOCATION OF ROUTING | $S_2S_1$ | LAYER | $Y_1Y_2$ | $Y_1Y_3$ | $Y_1Y_4$ | $X_1X_2$ | $X_1X_3$ | $X_1X_4$ |
| 200 mil CHANNEL[2] | 24% | $P/S_1$ | 34% | 12% | 8.0% | 32% | 20% | 20% |
| | | $G/S_2$ | 34 | 12 | 8.0 | | | |
| 100 mil CHANNEL | 19 | $P/S_1$ | — | — | — | — | — | — |
| | | $G/S_2$ | — | — | — | | | |

CONDUCTOR WIDTH = 8 mils, CONDUCTOR SPACING = 9 mils

| | INTERLAYER | INTRALAYER | | | | ALTERNATELY ON $P/S_1$, $G/S_2$ | | |
|---|---|---|---|---|---|---|---|---|
| LOCATION OF ROUTING | $S_2S_1$ | LAYER | $Y_1Y_2$ | $Y_1Y_3$ | $Y_1Y_4$ | $X_1X_2$ | $X_1X_3$ | $X_1X_4$ |
| 200 mil CHANNEL | 21% | $P/S_1$ | 39% | 17% | 10% | 34% | 22% | 22% |
| | | $G/S_2$ | 37 | 16 | 9.2 | | | |
| 100 mil CHANNEL | 17 | $P/S_1$ | 32 | — | — | 30 | — | — |
| | | $G/S_2$ | 32 | — | — | | | |

(1) CROSSTALK WAS MEASURED AS A PERCENTAGE OF THE SIGNAL STEP.

(2) THE P/G ROUTING ALSO OCCUPIES THE 200 mil CHANNELS.

(3) NO COVERCOAT CASE. COVERCOAT (GFR) INCREASES CROSSTALK BY ABOUT 10% OF THE TABULATED VALUES.

Fig. 6—Impedance, propagation delay, rise time, bandwidth, and pulse crosstalk for the double-sided epoxy printed wiring board with 963C-100 connectors.

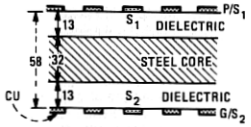


● 2 OZ CU CONDUCTORS ● ALL DIMENSIONS IN MILS

(a) NOTATION FOR INTERLAYER CROSSTALK ON THE DOUBLE SIDED METAL PWB.

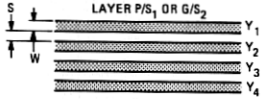


(b) NOTATION FOR INTRALAYER CROSSTALK. W = 12, S = 13 MILS OR W = 8, S = 9 MILS.

**TABLE A**
**PULSE TRANSMISSION PROPERTIES OF THE DOUBLE–SIDED METAL PWB[3]**

| | CONDUCTOR WIDTH = 12 mils CONDUCTOR SPACING = 13 mils | | CONDUCTOR WIDTH = 8 mils CONDUCTOR SPACING = 9 mils | |
|---|---|---|---|---|
| | SIGNAL LAYER | CHARACTERISTIC IMPEDANCE (OHMS) | SIGNAL LAYER | CHARACTERISTIC IMPEDANCE (OHMS) |
| ROUTING IN 200 mil CHANNELS[2] | $P/S_1$ | 89 OHMS | $P/S_1$ | 104 OHMS |
| | $G/S_2$ | 85 | $G/S_2$ | 106 |
| | $P/S_1 \rightarrow G/S_2$[1] | 77 | $P/S_1 \rightarrow G/S_2$ | 92 |
| ROUTING IN 100 mil CHANNELS | $P/S_1$ | 87 | $P/S_1$ | 104 |
| | $G/S_2$ | 83 | $G/S_2$ | 104 |
| | $P/S_1 \rightarrow G/S_2$ | 78 | $P/S_1 \rightarrow G/S_2$ | 90 |

- PROPAGATION DELAY = 1.5 ns/ft. (=1/v).
- 80% RISE TIME ON TDR FOR 1 ft. CONDUCTOR LENGTH = 2.6 ns.
- BANDWIDTH FOR 1 ft. CONDUCTOR LENGTH = 190 MHz.

(1) THE TRANSITIONS FROM $P/S_1$ TO $G/S_2$ USED 10 VIAS.

(2) THE P/G ROUTING ALSO OCCUPIES THE 200 mil CHANNELS.

(3) NO COVERCOAT CASE. COVERCOAT (GFR) HAS NEGLIGIBLE EFFECT ON RISE TIME (OR BANDWIDTH) BUT DECREASES THE CHARACTERISTIC IMPEDANCE BY ABOUT 5% AND INCREASES THE PROPAGATION DELAY BY ABOUT 10%.

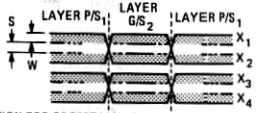


(c) NOTATION FOR CROSSTALK BETWEEN CONDUCTORS WHICH APPEAR ALTERNATELY ON LAYERS $P/S_1$ AND $G/S_2$. W = 12, S = 13 MILS OR W = 8, S = 9 MILS.

**TABLE B**
**$K_{ne}$ = MAXIMUM NEAR–END PULSE CROSSTALK[1] FOR VARIOUS CONDUCTOR PAIRS ON THE DOUBLE–SIDED METAL PWB[3]**

CONDUCTOR WIDTH = 12 mils, CONDUCTOR SPACING = 13 mils

| | INTERLAYER | INTRALAYER | | | | ALTERNATELY ON $P/S_1$, $G/S_2$ | | |
|---|---|---|---|---|---|---|---|---|
| LOCATION OF ROUTING | $S_2 S_1$ | LAYER | $Y_1 Y_2$ | $Y_1 Y_3$ | $Y_1 Y_4$ | $X_1 X_2$ | $X_1 X_3$ | $X_1 X_4$ |
| 200 mil CHANNEL[2] | 3.2% | $P/S_1$ | 13% | 2.8% | 0.8% | 9.2% | 2.4% | 6.8% |
| | | $G/S_2$ | 13 | 2.4 | 0.8 | | | |
| 100 mil CHANNEL | 1.2 | $P/S_1$ | — | — | — | — | — | — |
| | | $G/S_2$ | — | — | — | | | |

CONDUCTOR WIDTH = 8 mils, CONDUCTOR SPACING = 9 mils

| | INTERLAYER | INTRALAYER | | | | ALTERNATELY ON $P/S_1$, $G/S_2$ | | |
|---|---|---|---|---|---|---|---|---|
| LOCATION OF ROUTING | $S_2 S_1$ | LAYER | $Y_1 Y_2$ | $Y_1 Y_3$ | $Y_1 Y_4$ | $X_1 X_2$ | $X_1 X_3$ | $X_1 X_4$ |
| 200 mil CHANNEL | 1.2% | $P/S_1$ | 15% | 3.6% | 1.2% | 11% | 3.2% | 8.0% |
| | | $G/S_2$ | 14 | 3.2 | 1.2 | | | |
| 100 mil CHANNEL | 1.2 | $P/S_1$ | 14 | — | — | 11 | — | — |
| | | $G/S_2$ | 13 | — | — | | | |

(1) CROSSTALK WAS MEASURED AS A PERCENTAGE OF THE SIGNAL STEP.

(2) THE P/G ROUTING ALSO OCCUPIES THE 200 mil CHANNELS.

(3) NO COVERCOAT CASE. COVERCOAT (GFR) INCREASES CROSSTALK BY ABOUT 10% OF THE TABULATED VALUES.

Fig. 7—Impedance, propagation delay, rise time, bandwidth, and pulse crosstalk for the double-sided metal printed wiring board with 963C-100 connectors.

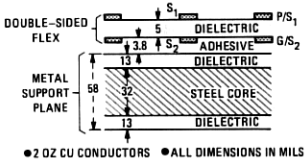


●2 OZ CU CONDUCTORS ●ALL DIMENSIONS IN MILS

(a) NOTATION FOR INTERLAYER CROSSTALK ON THE BONDED BOARD.

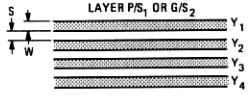


(b) NOTATION FOR INTRALAYER CROSSTALK.
W = 12, S = 13 MILS OR W = 8, S = 9 MILS.

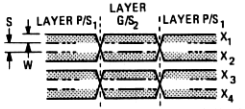


(c) NOTATION FOR CROSSTALK BETWEEN CONDUCTORS WHICH APPEAR ALTERNATELY ON LAYERS $P/S_1$ AND $G/S_2$.
W = 12, S = 13 MILS OR W = 8, S = 9 MILS.

**TABLE A**
**PULSE TRANSMISSION PROPERTIES OF THE BONDED BOARD[3]**

| | CONDUCTOR WIDTH = 12 mils CONDUCTOR SPACING = 13 mils | | CONDUCTOR WIDTH = 8 mils CONDUCTOR SPACING = 9 mils | |
|---|---|---|---|---|
| | SIGNAL LAYER | CHARACTERISTIC IMPEDANCE (OHMS) | SIGNAL LAYER | CHARACTERISTIC IMPEDANCE (OHMS) |
| ROUTING IN 200 mil CHANNELS[2] | $P/S_1$ | 95 OHMS | $P/S_1$ | 104 OHMS |
| | $G/S_2$ | 84 | $G/S_2$ | 89 |
| | $P/S_1 \rightarrow G/S_2$[1] | 77 | $P/S_1 \rightarrow G/S_2$ | 88 |
| ROUTING IN 100 mil CHANNELS | $P/S_1$ | 89 | $P/S_1$ | 102 |
| | $G/S_2$ | 73 | $G/S_2$ | 84 |
| | $P/S_1 \rightarrow G/S_2$ | 82 | $P/S_1 \rightarrow G/S_2$ | 97 |

● PROPAGATION DELAY = 1.5 ns/ft. (=1/v).
● 80% RISE TIME ON TDR FOR 1 ft. CONDUCTOR LENGTH = 2.6 ns.
● BANDWIDTH FOR 1 ft. CONDUCTOR LENGTH = 190 MHz.

(1) THE TRANSITIONS FROM $P/S_1$ TO $G/S_2$ USED 10 VIAS.

(2) THE P/G ROUTING ALSO OCCUPIES THE 200 mil CHANNELS.

(3) NO COVERCOAT CASE. COVERCOAT (GFR) HAS NEGLIGIBLE EFFECT ON RISE TIME (OR BANDWIDTH) BUT DECREASES THE CHARACTERISTIC IMPEDANCE BY ABOUT 5% AND INCREASES THE PROPAGATION DELAY BY ABOUT 10%.

**TABLE B**
**$K_{ne}$ = MAXIMUM NEAR-END PULSE CROSSTALK[1] FOR VARIOUS CONDUCTOR PAIRS ON THE BONDED BOARD[3]**

CONDUCTOR WIDTH = 12 mils, CONDUCTOR SPACING = 13 mils

| | INTERLAYER | INTRALAYER | | | | ALTERNATELY ON $P/S_1$, $G/S_2$ | | |
|---|---|---|---|---|---|---|---|---|
| LOCATION OF ROUTING | $S_2 S_1$ | LAYER | $Y_1 Y_2$ | $Y_1 Y_3$ | $Y_1 Y_4$ | $X_1 X_2$ | $X_1 X_3$ | $X_1 X_4$ |
| 200 mil CHANNEL[2] | 44% | $P/S_1$ | 19% | 4.0% | 1.2% | 16% | 6.4% | 7.6% |
| | | $G/S_2$ | 19 | 3.6 | 1.2 | | | |
| 100 mil CHANNEL | 40 | $P/S_1$ | — | — | — | — | — | — |
| | | $G/S_2$ | — | — | — | | | |

CONDUCTOR WIDTH = 8 mils, CONDUCTOR SPACING = 9 mils

| | INTERLAYER | INTRALAYER | | | | ALTERNATELY ON $P/S_1$, $G/S_2$ | | |
|---|---|---|---|---|---|---|---|---|
| LOCATION OF ROUTING | $S_2 S_1$ | LAYER | $Y_1 Y_2$ | $Y_1 Y_3$ | $Y_1 Y_4$ | $X_1 X_2$ | $X_1 X_3$ | $X_1 X_4$ |
| 200 mil CHANNEL | 38% | $P/S_1$ | 21% | 7.2% | 3.2% | 20% | 8.4% | 11% |
| | | $G/S_2$ | 21 | 6.8 | 3.2 | | | |
| 100 mil CHANNEL | 38 | $P/S_1$ | 20 | — | — | 21 | — | — |
| | | $G/S_2$ | 20 | — | — | | | |

(1) CROSSTALK WAS MEASURED AS A PERCENTAGE OF THE SIGNAL STEP.

(2) THE P/G ROUTING ALSO OCCUPIES THE 200 mil CHANNELS.

(3) NO COVERCOAT CASE. COVERCOAT (GFR) INCREASES INTRALAYER CROSSTALK BY ABOUT 10% OF THE TABULATED VALUES.

Fig. 8—Impedance, propagation delay, rise time, bandwidth, and pulse crosstalk for the bonded board with 963C-100 connectors.

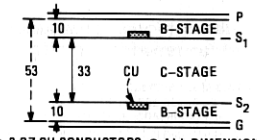


● 2 OZ CU CONDUCTORS ● ALL DIMENSIONS IN MILS

(a) NOTATION FOR INTERLAYER CROSSTALK ON THE 4L MLB (EXT P/G).

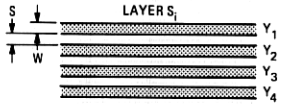


(b) NOTATION FOR INTRALAYER CROSSTALK. W = 12, S = 13 MILS OR W = 8, S = 9 MILS.

**TABLE A**
**PULSE TRANSMISSION PROPERTIES OF THE 4L MLB (EXT P/G)**

| | CONDUCTOR WIDTH = 12 mils CONDUCTOR SPACING = 13 mils | | CONDUCTOR WIDTH = 8 mils CONDUCTOR SPACING = 9 mils | |
|---|---|---|---|---|
| | SIGNAL LAYER | CHARACTERISTIC IMPEDANCE (OHMS) | SIGNAL LAYER | CHARACTERISTIC IMPEDANCE (OHMS) |
| ROUTING IN 200 mil CHANNELS(2) | $S_1$ | 58 OHMS | $S_1$ | 61 OHMS |
| | $S_2$ | 56 | $S_2$ | 64 |
| | $S_1 \rightarrow S_2$ (1) | 54 | $S_1 \rightarrow S_2$ | 64 |
| ROUTING IN 100 mil CHANNELS | $S_1$ | 117 | $S_1$ | 129 |
| | $S_2$ | 117 | $S_2$ | 129 |
| | $S_1 \rightarrow S_2$ | 111 | $S_1 \rightarrow S_2$ | 120 |

● PROPAGATION DELAY = 1.8 ns/ft. (=1/v).
● 80% RISE TIME ON TDR FOR 1 ft. CONDUCTOR LENGTH = 2.5 ns.
● BANDWIDTH FOR 1 ft. CONDUCTOR LENGTH = 200 MHz.

(1) THE TRANSITIONS FROM $S_1$ TO $S_2$ USED 10 VIAS.
(2) THE EXTERNAL P/G ROUTING ALSO OCCUPIES THE 200 mil CHANNELS.

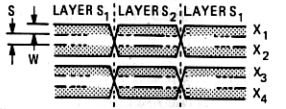


(c) NOTATION FOR CROSSTALK BETWEEN CONDUCTORS WHICH APPEAR ALTERNATELY ON LAYERS $S_1$ AND $S_2$. W = 12, S = 13 MILS OR W = 8, S = 9 MILS.

**TABLE B**
**$K_{ne}$ = MAXIMUM NEAR–END PULSE CROSSTALK(1) FOR VARIOUS CONDUCTOR PAIRS ON THE 4L MLB (EXT P/G)**

CONDUCTOR WIDTH = 12 mils, CONDUCTOR SPACING = 13 mils

| | INTERLAYER | INTRALAYER | | | | ALTERNATELY ON $S_1$, $S_2$ | | |
|---|---|---|---|---|---|---|---|---|
| LOCATION OF ROUTING | $S_2$ $S_1$ | LAYER | $Y_1$ $Y_2$ | $Y_1$ $Y_3$ | $Y_1$ $Y_4$ | $X_1$ $X_2$ | $X_1$ $X_3$ | $X_1$ $X_4$ |
| 200 mil CHANNEL(2) | 13% | $S_1$ | 16% | 9.2% | 8.4% | 14% | 9.0% | 8.0% |
| | | $S_2$ | 14 | 11 | 8.4 | | | |
| 100 mil CHANNEL | 21 | $S_1$ | — | — | — | — | — | — |
| | | $S_2$ | — | — | — | | | |

CONDUCTOR WIDTH = 8 mils, CONDUCTOR SPACING = 9 mils

| | INTERLAYER | INTRALAYER | | | | ALTERNATELY ON $S_1$, $S_2$ | | |
|---|---|---|---|---|---|---|---|---|
| LOCATION OF ROUTING | $S_2$ $S_1$ | LAYER | $Y_1$ $Y_2$ | $Y_1$ $Y_3$ | $Y_1$ $Y_4$ | $X_1$ $X_2$ | $X_1$ $X_3$ | $X_1$ $X_4$ |
| 200 mil CHANNEL | 12% | $S_1$ | 16% | 10% | 8.4% | 13% | 7.2% | 8.8% |
| | | $S_2$ | 16 | 12 | 8.4 | | | |
| 100 mil CHANNEL | 20 | $S_1$ | 31 | — | — | 28 | — | — |
| | | $S_2$ | 30 | — | — | | | |

(1) CROSSTALK WAS MEASURED AS A PERCENTAGE OF THE SIGNAL STEP.
(2) THE EXTERNAL P/G ROUTING ALSO OCCUPIES THE 200 mil CHANNELS.

Fig. 9—Impedance, propagation delay, rise time, bandwidth, and pulse crosstalk for the 4L MLB (EXT P/G) with 963C-100 connectors.

(a) NOTATION FOR INTERLAYER CROSSTALK ON THE 6L MLB (EXT P/G).

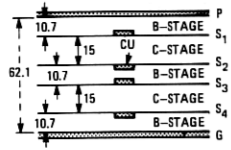


● 2 OZ CU CONDUCTORS ● ALL DIMENSIONS IN MILS

(b) NOTATION FOR INTRALAYER CROSSTALK. W = 12, S = 13 MILS OR W = 8, S = 9 MILS.

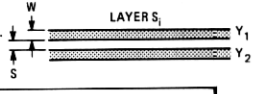


**TABLE A**
**PULSE TRANSMISSION PROPERTIES OF THE 6L MLB (EXT P/G)**

| | CONDUCTOR WIDTH = 12 mils CONDUCTOR SPACING = 13 mils | | CONDUCTOR WIDTH = 8 mils CONDUCTOR SPACING = 9 mils | |
|---|---|---|---|---|
| | SIGNAL LAYER | CHARACTERISTIC IMPEDANCE (OHMS) | SIGNAL LAYER | CHARACTERISTIC IMPEDANCE (OHMS) |
| ROUTING IN 200 mil CHANNELS(2) | $S_1$ | 36 OHMS | $S_1$ | 43 OHMS |
| | $S_2$ | 64 | $S_2$ | 68 |
| | $S_3$ | 61 | $S_3$ | 62 |
| | $S_4$ | 39 | $S_4$ | 47 |
| | $S_1 \rightarrow S_4$(1) | 44 | $S_1 \rightarrow S_4$ | 52 |
| ROUTING IN 100 mil CHANNELS | $S_1$ | 102 | $S_1$ | 104 |
| | $S_2$ | 95 | $S_2$ | 106 |
| | $S_3$ | 95 | $S_3$ | 97 |
| | $S_4$ | 104 | $S_4$ | 106 |
| | $S_1 \rightarrow S_4$ | 99 | $S_1 \rightarrow S_4$ | 103 |

● PROPAGATION DELAY = 1.8 ns/ft. (=1/v).
● 80% RISE TIME ON TDR FOR 1 ft. CONDUCTOR LENGTH = 2.5 ns.
● BANDWIDTH FOR 1 ft. CONDUCTOR LENGTH = 200 MHz.

(1) THE TRANSITIONS FROM $S_1$ TO $S_4$ USED 5 OR 10 VIAS.

(2) THE EXTERNAL P/G ROUTING ALSO OCCUPIES THE 200 mil CHANNELS.

(c) NOTATION FOR CROSSTALK BETWEEN CONDUCTORS WHICH APPEAR ALTERNATELY ON LAYERS $S_1$ AND $S_4$. W = 12, S = 13 MILS OR W = 8, S = 9 MILS.

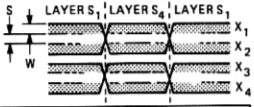


**TABLE B**
**$K_{ne}$ = MAXIMUM NEAR–END PULSE CROSSTALK(1) FOR VARIOUS CONDUCTOR PAIRS ON THE 6L MLB (EXT P/G)**

CONDUCTOR WIDTH = 12 mils, CONDUCTOR SPACING = 13 mils

| | INTERLAYER | | | INTRALAYER | | ALTERNATELY ON $S_1$, $S_4$ | | |
|---|---|---|---|---|---|---|---|---|
| LOCATION OF ROUTING | $S_2S_1$ | $S_2S_3$ | $S_2S_4$ | LAYER | $Y_1Y_2$ | $X_1X_2$ | $X_1X_3$ | $X_1X_4$ |
| 200 mil CHANNEL(2) | 12% | 35% | 5.0% | $S_1$ | 11% | 16% | 7.2% | 8.0% |
| | | | | $S_2$ | 14 | | | |
| | | | | $S_3$ | 16 | | | |
| | | | | $S_4$ | 16 | | | |
| 100 mil CHANNEL | 32 | 46 | 16 | $S_1$ | — | — | — | — |
| | | | | $S_2$ | — | | | |
| | | | | $S_3$ | — | | | |
| | | | | $S_4$ | — | | | |

CONDUCTOR WIDTH = 8 mils, CONDUCTOR SPACING = 9 mils

| | INTERLAYER | | | INTRALAYER | | ALTERNATELY ON $S_1$, $S_4$ | | |
|---|---|---|---|---|---|---|---|---|
| LOCATION OF ROUTING | $S_2S_1$ | $S_2S_3$ | $S_2S_4$ | LAYER | $Y_1Y_2$ | $X_1X_2$ | $X_1X_3$ | $X_1X_4$ |
| 200 mil CHANNEL | 8.0% | 30% | 5.0% | $S_1$ | 17% | 16% | 13% | 14% |
| | | | | $S_2$ | 20 | | | |
| | | | | $S_3$ | 20 | | | |
| | | | | $S_4$ | 18 | | | |
| 100 mil CHANNEL | 28 | 40 | 13 | $S_1$ | 31 | 29 | — | — |
| | | | | $S_2$ | 32 | | | |
| | | | | $S_3$ | 32 | | | |
| | | | | $S_4$ | 32 | | | |

(1) CROSSTALK WAS MEASURED AS A PERCENTAGE OF THE SIGNAL STEP.

(2) THE EXTERNAL P/G ROUTING ALSO OCCUPIES THE 200 mil CHANNELS.

Fig. 10—Impedance, propagation delay, rise time, bandwidth, and pulse crosstalk for the 6L MLB (EXT P/G) with 963C-100 connectors.

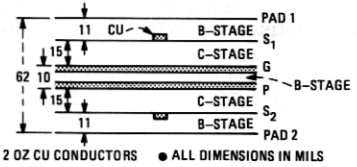


● 2 OZ CU CONDUCTORS ● ALL DIMENSIONS IN MILS

(a) NOTATION FOR INTERLAYER CROSSTALK ON THE 6L MLB (INT P/G).

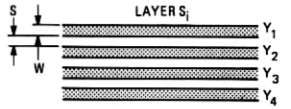


(b) NOTATION FOR INTRALAYER CROSSTALK W = 12, S = 13 MILS OR W = 8, S = 9 MILS.

**TABLE A**
**PULSE TRANSMISSION PROPERTIES OF THE 6L MLB (INT P/G)**

| | CONDUCTOR WIDTH = 12 mils CONDUCTOR SPACING = 13 mils | | CONDUCTOR WIDTH = 8 mils CONDUCTOR SPACING = 9 mils | |
|---|---|---|---|---|
| | SIGNAL LAYER | CHARACTERISTIC IMPEDANCE (OHMS) | SIGNAL LAYER | CHARACTERISTIC IMPEDANCE (OHMS) |
| ROUTING IN 200 mil CHANNELS | $S_1$ | 61 OHMS | $S_1$ | 72 OHMS |
| | $S_2$ | 62 | $S_2$ | 70 |
| | $S_1 \rightarrow S_2$ (1) | 60 | $S_1 \rightarrow S_2$ | 64 |
| ROUTING IN 100 mil CHANNELS | $S_1$ | 64 | $S_1$ | 71 |
| | $S_2$ | 64 | $S_2$ | 68 |
| | $S_1 \rightarrow S_2$ | 58 | $S_1 \rightarrow S_2$ | 65 |

- PROPAGATION DELAY = 1.9 ns/ft. (= 1/v).
- 80% RISE TIME ON TDR FOR 1 ft. CONDUCTOR LENGTH = 1.8 ns.
- BANDWIDTH FOR 1 ft. CONDUCTOR LENGTH = 278 MHz.

(1) THE TRANSITIONS FROM $S_1$ TO $S_2$ USED 10 VIAS.

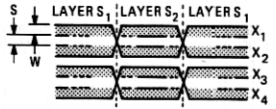


(c) NOTATION FOR CROSSTALK BETWEEN CONDUCTORS WHICH APPEAR ALTERNATELY ON LAYERS $S_1$ AND $S_2$. W = 12, S = 13 MILS OR W = 8, S = 9 MILS.

**TABLE B**
**$K_{ne}$ = MAXIMUM NEAR–END PULSE CROSSTALK(1) FOR VARIOUS CONDUCTOR PAIRS ON THE 6L MLB (INT P/G)**

| CONDUCTOR WIDTH = 12 mils, CONDUCTOR SPACING = 13 mils | | | | | | | | |
|---|---|---|---|---|---|---|---|---|
| | INTERLAYER | INTRALAYER | | | | ALTERNATELY ON $S_1, S_2$ | | |
| LOCATION OF ROUTING | $S_2 S_1$ | LAYER | $Y_1 Y_2$ | $Y_1 Y_3$ | $Y_1 Y_4$ | $X_1 X_2$ | $X_1 X_3$ | $X_1 X_4$ |
| 200 mil CHANNEL | 0.5% | $S_1$ | 15% | 3.0% | 2.0% | 12% | 5.2% | 6.4% |
| | | $S_2$ | 14 | 2.9 | 1.2 | | | |
| 100 mil CHANNEL | 0.5% | $S_1$ | — | — | — | — | — | — |
| | | $S_2$ | — | — | — | | | |
| CONDUCTOR WIDTH = 8 mils, CONDUCTOR SPACING = 9 mils | | | | | | | | |
| | INTERLAYER | INTRALAYER | | | | ALTERNATELY ON $S_1, S_2$ | | |
| LOCATION OF ROUTING | $S_2 S_1$ | LAYER | $Y_1 Y_2$ | $Y_1 Y_3$ | $Y_1 Y_4$ | $X_1 X_2$ | $X_1 X_3$ | $X_1 X_4$ |
| 200 mil CHANNEL | 0.4% | $S_1$ | 20% | 5.0% | 2.4% | 16% | 5.2% | 6.8% |
| | | $S_2$ | 20 | 5.0 | 2.0 | | | |
| 100 mil CHANNEL | 0.4 | $S_1$ | 20 | — | — | 16 | — | — |
| | | $S_2$ | 20 | — | — | | | |

(1) CROSSTALK WAS MEASURED AS A PERCENTAGE OF THE SIGNAL STEP.

Fig. 11—Impedance, propagation delay, rise time, bandwidth, and pulse crosstalk for the 6L MLB (INT P/G) with 963C-100 connectors.

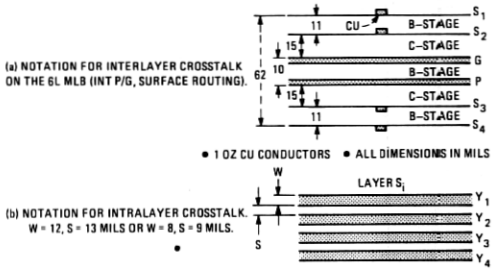


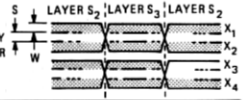


**TABLE A**
**PULSE TRANSMISSION PROPERTIES OF THE 6L MLB (INT P/G, SURFACE ROUTING)[2]**

| | CONDUCTOR WIDTH = 12 mils CONDUCTOR SPACING = 13 mils | | CONDUCTOR WIDTH = 8 mils CONDUCTOR SPACING = 9 mils | |
|---|---|---|---|---|
| | SIGNAL LAYER | CHARACTERISTIC IMPEDANCE (OHMS) | SIGNAL LAYER | CHARACTERISTIC IMPEDANCE (OHMS) |
| ROUTING IN 200 mil CHANNELS | $S_1$ | 89 OHMS | $S_1$ | 104 OHMS |
| | $S_2$ | 66 | $S_2$ | 72 |
| | $S_3$ | 66 | $S_3$ | 75 |
| | $S_4$ | 92 | $S_4$ | 110 |
| | $S_2 \rightarrow S_3$[1] | 59 | $S_2 \rightarrow S_3$ | 65 |
| ROUTING IN 100 mil CHANNELS | $S_1$ | 92 | $S_1$ | 106 |
| | $S_2$ | 69 | $S_2$ | 73 |
| | $S_3$ | 68 | $S_3$ | 75 |
| | $S_4$ | 93 | $S_4$ | 109 |
| | $S_2 \rightarrow S_3$ | 60 | $S_2 \rightarrow S_3$ | 66 |

- PROPAGATION DELAY = 1.5 ns/ft. (= 1/v) ON $S_1, S_4$ AND 1.8 ns/ft. (= 1/v) ON $S_2, S_3$.
- 80% RISE TIME ON TDR FOR 1 ft. CONDUCTOR LENGTH = 1.8 ns.
- BANDWIDTH FOR 1 ft. CONDUCTOR LENGTH = 278 MHz.

(1) THE TRANSITIONS FROM $S_2$ TO $S_3$ USED 10 VIAS.
(2) NO COVERCOAT CASE. ON LAYERS $S_1, S_4$, COVERCOAT (GFR) HAS NEGLIGIBLE EFFECT ON RISE TIME (OR BANDWIDTH) BUT DECREASES THE CHARACTERISTIC IMPEDANCE BY ABOUT 10% AND INCREASES THE PROPAGATION DELAY BY ABOUT 10%.

**TABLE B**
**$K_{ne}$ = MAXIMUM NEAR-END PULSE CROSSTALK[1] FOR VARIOUS CONDUCTOR PAIRS ON THE 6L MLB (INT P/G, SURFACE ROUTING)[2]**

CONDUCTOR WIDTH = 12 mils, CONDUCTOR SPACING = 13 mils

| | INTERLAYER | | INTRALAYER | | | | ALTERNATELY ON $S_2, S_3$ | | |
|---|---|---|---|---|---|---|---|---|---|
| LOCATION OF ROUTING | $S_1 S_2$ | $S_3 S_4$ | LAYER | $Y_1 Y_2$ | $Y_1 Y_3$ | $Y_1 Y_4$ | $X_1 X_2$ | $X_1 X_3$ | $X_1 X_4$ |
| 200 mil CHANNEL | 25% | 25% | $S_1$ | 14% | 4% | 1.8% | 9.2% | 2.8% | 5.0% |
| | | | $S_2$ | 12 | 3.2 | 1.7 | | | |
| | | | $S_3$ | 12 | 3.0 | 1.1 | | | |
| | | | $S_4$ | 14 | 4.0 | 1.7 | | | |
| 100 mil CHANNEL | 26 | 26 | $S_1$ | — | — | — | — | — | — |
| | | | $S_2$ | — | — | — | | | |
| | | | $S_3$ | — | — | — | | | |
| | | | $S_4$ | — | — | — | | | |

CONDUCTOR WIDTH = 8 mils, CONDUCTOR SPACING = 9 mils

| | INTERLAYER | | INTRALAYER | | | | ALTERNATELY ON $S_2, S_3$ | | |
|---|---|---|---|---|---|---|---|---|---|
| LOCATION OF ROUTING | $S_1 S_2$ | $S_3 S_4$ | LAYER | $Y_1 Y_2$ | $Y_1 Y_3$ | $Y_1 Y_4$ | $X_1 X_2$ | $X_1 X_3$ | $X_1 X_4$ |
| 200 mil CHANNEL | 22% | 22% | $S_1$ | 16% | 5.8% | 3.1% | 12% | 3.8% | 7.1% |
| | | | $S_2$ | 16 | 4.5 | 2.0 | | | |
| | | | $S_3$ | 16 | 5.3 | 2.0 | | | |
| | | | $S_4$ | 16 | 5.6 | 2.5 | | | |
| 100 mil CHANNEL | 21 | 22 | $S_1$ | 16 | — | — | 13 | — | — |
| | | | $S_2$ | 16 | — | — | | | |
| | | | $S_3$ | 16 | — | — | | | |
| | | | $S_4$ | 16 | — | — | | | |

(1) CROSSTALK WAS MEASURED AS A PERCENTAGE OF THE SIGNAL STEP.
(2) NO COVERCOAT CASE. ON LAYERS $S_1, S_4$, COVERCOAT (GFR) INCREASES INTRALAYER CROSSTALK BY ABOUT 20% OF THE TABULATED VALUES.

Fig. 12—Impedance, propagation delay, rise time, bandwidth, and pulse crosstalk for the 6L MLB (INT P/G, surface routing) with 963C-100 connectors.

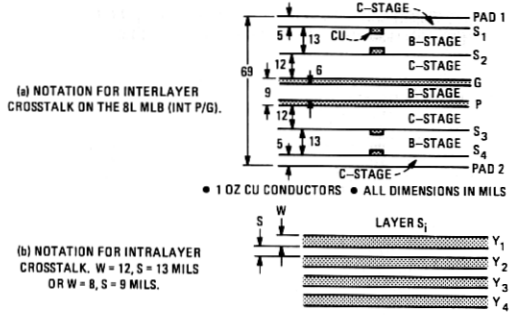


(a) NOTATION FOR INTERLAYER CROSSTALK ON THE 8L MLB (INT P/G).

(b) NOTATION FOR INTRALAYER CROSSTALK. W = 12, S = 13 MILS OR W = 8, S = 9 MILS.

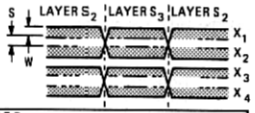


(c) NOTATION FOR CROSSTALK BETWEEN CONDUCTORS WHICH APPEAR ALTERNATELY ON LAYERS $S_2$ AND $S_3$. W = 12, S = 13 MILS OR W = 8, S = 9 MILS.

**TABLE A**
**PULSE TRANSMISSION PROPERTIES OF THE 8L MLB (INT P/G)**

| | CONDUCTOR WIDTH = 12 mils CONDUCTOR SPACING = 13 mils | | CONDUCTOR WIDTH = 8 mils CONDUCTOR SPACING = 9 mils | |
|---|---|---|---|---|
| | SIGNAL LAYER | CHARACTERISTIC IMPEDANCE (OHMS) | SIGNAL LAYER | CHARACTERISTIC IMPEDANCE (OHMS) |
| ROUTING IN 200 mil CHANNELS | $S_1$ | 94 OHMS | $S_1$ | 114 OHMS |
| | $S_2$ | 65 | $S_2$ | 83 |
| | $S_3$ | 68 | $S_3$ | 82 |
| | $S_4$ | 85 | $S_4$ | 102 |
| | $S_2 \rightarrow S_3$ (1) | 62 | $S_2 \rightarrow S_3$ | 73 |
| ROUTING IN 100 mil CHANNELS | $S_1$ | 91 | $S_1$ | 111 |
| | $S_2$ | 65 | $S_2$ | 84 |
| | $S_3$ | 68 | $S_3$ | 83 |
| | $S_4$ | 84 | $S_4$ | 102 |
| | $S_2 \rightarrow S_3$ | 62 | $S_2 \rightarrow S_3$ | 74 |

- PROPAGATION DELAY = 1.9 ns/ft. (= 1/v).
- 80% RISE TIME ON TDR FOR 1 ft. CONDUCTOR LENGTH = 1.8 ns.
- BANDWIDTH FOR 1 ft. CONDUCTOR LENGTH = 278 MHz.

(1) THE TRANSITIONS FROM $S_2$ TO $S_3$ USED 10 VIAS.

**TABLE B**
**$K_{ne}$ = MAXIMUM NEAR–END PULSE CROSSTALK(1) FOR VARIOUS CONDUCTOR PAIRS ON THE 8L MLB (INT P/G)**

CONDUCTOR WIDTH = 12 mils, CONDUCTOR SPACING = 13 mils

| | INTERLAYER | | INTRALAYER | | | | ALTERNATELY ON $S_2, S_3$ | | |
|---|---|---|---|---|---|---|---|---|---|
| LOCATION OF ROUTING | $S_1 S_2$ | $S_3 S_4$ | LAYER | $Y_1 Y_2$ | $Y_1 Y_3$ | $Y_1 Y_4$ | $X_1 X_2$ | $X_1 X_3$ | $X_1 X_4$ |
| 200 mil CHANNEL | 20% | 24% | $S_1$ | 12% | 3.2% | 1.3% | 6.8% | 2.5% | 3.3% |
| | | | $S_2$ | 8.4 | 1.8 | 0.8 | | | |
| | | | $S_3$ | 9.2 | 1.9 | 1.1 | | | |
| | | | $S_4$ | 12 | 3.2 | 1.3 | | | |
| 100 mil CHANNEL | 20 | 24 | $S_1$ | — | — | — | — | — | — |
| | | | $S_2$ | — | — | — | | | |
| | | | $S_3$ | — | — | — | | | |
| | | | $S_4$ | — | — | — | | | |

CONDUCTOR WIDTH = 8 mils, CONDUCTOR SPACING = 9 mils

| | INTERLAYER | | INTRALAYER | | | | ALTERNATELY ON $S_2 S_3$ | | |
|---|---|---|---|---|---|---|---|---|---|
| LOCATION OF ROUTING | $S_1 S_2$ | $S_3 S_4$ | LAYER | $Y_1 Y_2$ | $Y_1 Y_3$ | $Y_1 Y_4$ | $X_1 X_2$ | $X_1 X_3$ | $X_1 X_4$ |
| 200 mil CHANNEL | 19% | 20% | $S_1$ | 16% | 5.2% | 2.4% | 9.2% | 2.8% | 5.2% |
| | | | $S_2$ | 12 | 3.6 | 2.0 | | | |
| | | | $S_3$ | 12 | 3.6 | 1.6 | | | |
| | | | $S_4$ | 18 | 5.6 | 2.4 | | | |
| 100 mil CHANNEL | 18 | 20 | $S_1$ | 15 | — | — | 10 | — | — |
| | | | $S_2$ | 12 | — | — | | | |
| | | | $S_3$ | 12 | — | — | | | |
| | | | $S_4$ | 16 | — | — | | | |

(1) CROSSTALK WAS MEASURED AS A PERCENTAGE OF THE SIGNAL STEP.

Fig. 13—Impedance, propagation delay, rise time, bandwidth, and pulse crosstalk for the 8L MLB (INT P/G) with 963C-100 connectors.

## REFERENCES


1. Bell Laboratories, "*BELLPAC* User Guidelines," unpublished work.
2. A. J. Rainal, "Pulse Transmission Properties of Various Circuit Pack Configurations," unpublished work.
3. D. B. Jarvis, "The Effects of Interconnections on High Speed Logic Circuits," IEEE Trans. Elec. Computers, *EC-12*, No. 5 (October 1963), pp. 476–487.
4. H. R. Kaupp, "Pulse Crosstalk Between Microstrip Transmission Lines," 7th International Electronic Circuit Packaging Symposium, IECP 2/5, August 1966, pp. 1–12.
5. A. J. Rainal, R. C. Restrick, and J. N. Lahti, "1A Processor; Backplane Signal Propagation Experiments," unpublished work.
6. A. J. Rainal, "Electrical Guidelines on the Use of the 963 Connector for CDCP Applications," unpublished work.
7. P. I. Kuznetsov and R. L. Stratonovich, *The Propagation of Electromagnetic Waves in Multiconductor Transmission Lines, 1964*, New York: Pergamon Press, 1964.
8. J. C. Isaacs, Jr., and N. A. Strakhov, "Crosstalk in Uniformly Coupled Lossy Transmission Lines," B.S.T.J., *52*, No. 1 (January 1973), pp. 101–114.
9. H. S. Gray, *Digital Computer Engineering*, Englewood Cliffs, N.J.: Prentice-Hall, 1963.
10. A. Feller, H. R. Kaupp, and J. J. Digiacomo, "Crosstalk and Reflections in High-Speed Digital Systems," Proceedings—Fall Joint Computer Conference, December 1965, Washington, D. C.: Spartan Books, pp. 511–525.
11. N. C. Arvanitakis, J. T. Kolias, and W. Radzelovage, "Coupled Noise Prediction in Printed Circuit Boards for a High-Speed Computer System," 7th International Electronic Circuit Packaging Symposium, IECP 2/6, August 1966, pp. 1–11.
12. Bell Telephone Laboratories Staff, *Physical Design of Electronic Systems*, Vol. I, "Design Technology," Englewood Cliffs, N.J.: Prentice-Hall, 1970, pp. 389–392.
13. B. M. Oliver, "Directional Electromagnetic Coupling," Proc. IRE, *42*, No. 11 (November 1954), pp. 1686–1692.
14. G. A. Campbell, "Dr. Campbell's Memoranda of 1907 and 1912," B.S.T.J., *14*, No. 4 (October 1935), pp. 558–572.
15. S. A. Shelkunoff, and T. M. Odarenko, "Crosstalk Between Coaxial Transmission Lines," B.S.T.J., *16*, No. 2 (April 1937), pp. 144–164.